Structural Characterization of an Etheno-2‘-deoxyguanosine Adduct Modified by Tetrahydrofuran

ARTICLE *in* CHEMICAL RESEARCH IN TOXICOLOGY · MARCH 2005

Impact Factor: 3.53 · DOI: 10.1021/tx0497494 · Source: PubMed

6 AUTHORS, INCLUDING:

Ana Paula de Melo Loureiro
University of São Paulo
37 PUBLICATIONS **694** CITATIONS
SEE PROFILE

Osmar F Gomes
University of São Paulo
15 PUBLICATIONS **368** CITATIONS
SEE PROFILE

Paolo Di Mascio
University of São Paulo
237 PUBLICATIONS **7,277** CITATIONS
SEE PROFILE

Marisa H G Medeiros
University of São Paulo
151 PUBLICATIONS **3,657** CITATIONS
SEE PROFILE

Structural Characterization of an Etheno-2′-deoxyguanosine Adduct Modified by Tetrahydrofuran

Ana Paula M. Loureiro,[†] Ivan P. de Arruda Campos,[‡] Osmar F. Gomes,[§] Ediliz P. M. Possari,[†] Paolo Di Mascio,[§] and Marisa H. G. Medeiros*,[§]

Departamento de Análises Clínicas e Toxicológicas, Faculdade de Ciências Farmacêuticas, Universidade de São Paulo, Av. Prof. Lineu Prestes 580, Bloco 13 B, CEP 05508-900 São Paulo, Brazil, Programa de Pós-Graduação em Engenharia de Produção, Instituto de Ciências Exatas e Tecnologia, Universidade Paulista, Rua Dr. Bacelar 1212, CEP 04026−002 São Paulo, Brazil, and Departamento de Bioquímica, Instituto de Química, Universidade de São Paulo, Av. Prof. Lineu Prestes 748, CEP 05508-900 São Paulo, Brazil

Received September 8, 2004

The reaction of 2′-deoxyguanosine with the α,β-unsaturated aldehydes *trans*-2-octenal, *trans*-2-nonenal, *trans*-2-decenal, *trans*,*trans*-2,4-nonadienal, and *trans*,*trans*-2,4-decadienal in THF gives rise to three novel adducts: 3-(2′-deoxy-β-D-*erythro*-pentafuranosyl)-7-[3-hydroxy-1-(3-(2′-deoxy-β-D-*erythro*-pentafuranosyl)-3,5-dihydro-imidazo[1,2-*a*]purin-9-one-7-yl)-propyl]-3,5-dihydro-imidazo[1,2-*a*]purin-9-one (**A7**) and 3-(2′-deoxy-β-D-*erythro*-pentafuranosyl)-7-(tetrahydrofuran-2-yl)-3,5-dihydro-imidazo[1,2-*a*]purin-9-one (**A8** and **A9**), which are not observed in the absence of THF. These adducts were isolated from in vitro reactions by reversed-phase HPLC and fully characterized on the basis of spectroscopic measurements. Adduct **A7** consists of two 1,N^2-etheno-2′-deoxyguanosine (1,N^2-ϵdGuo) residues linked to a hydroxy-carbon side chain; adducts **A8** and **A9** are interconvertible 1,N^2-ϵdGuo derivatives bearing a THF moiety. The proposed reaction mechanism involves the electrophilic attack on 1,N^2-ϵdGuo by the carbonyl of 4-hydroxy-butanal, generated via ring opening of α-hydroxy-THF (THF−OH), yielding adducts **A8** and **A9**. A further combination of these adducts with another 1,N^2-ϵdGuo produces the double adduct **A7**. These findings demonstrate that reactions of unsaturated aldehydes in the presence of THF produce novel condensation 1,N^2-ϵdGuo-THF adducts. Further studies would indicate the relevance of these adducts in THF toxicity.

Introduction

Tetrahydrofuran (THF)[1] is a solvent used widely in industry and research. It is also a component of glues, paints, varnishes, and inks. In 1993, THF production in the United States was about 94.3×10^3 tons (*1*, *2*).

THF is a volatile solvent with a low boiling point. Therefore, high vapor concentrations may develop in the workplace with a strong potential for occupational exposure in humans. Ong and co-workers (*1*) investigated exposure to THF through vapor inhalation and dermal contact by analyzing the environmental air, blood, urine, and alveolar air of 58 male workers in a videotape manufacturing plant. For exposure at the time-weighted average (TWA) concentration of 200 ppm, the extrapolated concentration of THF was 33 μM in blood and 109 μM in urine. The end of shift urinary THF concentration correlated well with THF concentration in the environmental air and was proposed as a biological indicator for analyzing occupational exposure to THF (*1*). The symptoms following exposure may include nausea, headache, blurred vision, dizziness, tiredness, chest pain, and coughing. THF is an upper respiratory tract irritant, and irritation of skin and mucous membranes may be observed (*3*). Once in contact with air, THF may form peroxides, which increase its irritating effect. It is also a strong narcotic. Acute toxicity may lead to narcosis, muscular hypotonia, and disappearance of corneal reflexes, followed by coma and death. The probable oral lethal dose in humans is 50−500 mg/kg (*4*).

There is an emergent concern about human exposure to THF, since clear evidence was found of carcinogenic activity in female mice, based on the increased incidence of hepatocellular neoplasm after 2 years of exposure to 1800 ppm THF by inhalation (6 h/day, 5 days/week) (*4*, *5*). The nonobservable-adverse-effect level (NOAEL) for nonneoplastic lesions from THF is 600 ppm in mice after 14 weeks of exposure (6h/day, 5 days/week). However, in the 2-year study, even the incidence of hepatocellular neoplasm in female mice exposed to 200 ppm was elevated (48%) in relation to the controls (34%) (*4*, *5*). Considering that the current threshold limit value−time-

* To whom correspondence should be addressed. Tel: ++(55)11 30912153. Fax: ++(55)11 30912186. E-mail: mhgdmede@iq.usp.br.
[†] Faculdade de Ciências Farmacêuticas, Universidade de São Paulo.
[‡] Universidade Paulista.
[§] Instituto de Química, Universidade de São Paulo.

[1] Abbreviations: THF, tetrahydrofuran; TWA, time-weighted average; NOAEL, nonobservable-adverse-effect level; TLV−TWA, threshold limit value−time-weighted average; TLV−STEL, short-term exposure limit; dGuo, 2′-deoxyguanosine; DDE, *trans*,*trans*-2,4-decadienal; 1,N^2-ϵdGuo, 1,N^2-etheno-2′-deoxyguanosine; HPLC, high-performance liquid chromatography; ESI/MS, electrospray ionization mass spectrometry; SIR, selected ion recording; COSY, $^1H-^1H$ two-dimensional correlation spectroscopy; HMQC, $^1H-^{13}C$ two-dimensional heteronuclear multiple-quantum correlation; DEPT, distortionless enhancement by polarization transfer.

10.1021/tx0497494 CCC: $30.25
Published on Web 01/14/2005

weighted average (TLV−TWA) for THF is 200 ppm (590 mg/m^3) and the short-term exposure limit (TLV−STEL) is 250 ppm (737 mg/m^3) (*6*), the results obtained in the National Toxicology Program study (*4*) may have some implications for the current occupational exposure limit.

Although carcinogenic activity is observed in rodents, there is a paucity of information about cellular toxicity, biomolecular damage, and genotoxicity induced by THF. The limited information available from in vitro and in vivo genotoxicity studies points to THF as a nonmutagenic (*4*). However, further investigation is necessary to evaluate more precisely the possible interaction of THF oxidation products with biological targets such as DNA.

Our previous studies on DNA adducts from reaction of 2′-deoxyguanosine (dGuo) with *trans*,*trans*-2,4-decadienal (DDE) revealed the formation of three adducts that could be observed only in the reactions occurring in the presence of oxidized THF (*7*, *8*). The present data fully describe the structural characterization of these novel stable adducts produced by the reaction of THF oxidation products with 1,N^2-etheno-2′-deoxyguanosine (1,N^2-ϵdGuo). Information about the chemical pathways for adduct formation is also provided. The occurrence of an interaction leading to DNA−THF adducts may be a contributing factor to the observed toxicological effects associated with THF exposure.

Experimental Procedures

Chemicals. All the chemicals employed here were of the highest purity grade commercially available. *trans*-2-Octenal, *trans*-2-nonenal, *trans*-2-decenal, *trans*,*trans*-2,4-nonadienal, and DDE were supplied by Aldrich (Milwaukee, Wl). dGuo, formic acid, and potassium phosphate were acquired from Merck (Darmstadt, Germany). Chromatography grade acetonitrile, methanol, and THF were obtained from EM Science (Gibbstown, NJ). Chloroform was supplied by Cinética Química (São Paulo, Brazil). Oxidized THF was obtained from THF solvent unprotected from light. The concentration of hydroperoxides in the THF batches was measured by the Fe^{2+}/xylenol orange assay (*9*). 2-Hydroxy-THF was estimated by GC/flame ionization detector (FID) (HP5890). All the other chemicals used came from Sigma (St. Louis, MO). The water was purified in a Milli-Q system (Millipore, Bedford, MA).

Spectroscopy. One-dimensional (1D) and two-dimensional (2D) ^{1}H and ^{13}C NMR spectra were acquired at 27 °C using a DPX-300 or a DRX-500 MHz NMR spectrometer (Bruker, Rheinstatten, Germany). The samples were dissolved in DMSO-d_6, and the solvent peak was used as the reference. UV spectra were obtained with a Hitachi U3000 spectrophotometer (Tokyo, Japan).

HPLC Separations. HPLC analyses were made using a Shimadzu HPLC system (Shimadzu, Kyoto, Japan). This included two LC-10AD (or LC-10AD/VP) pumps, a Rheodyne injector (Cotati, CA), an SPD-10 AV absorbance device, and a SPD-M10AV (or SPD-M10A/VP) photodiode array detector, controlled by a CBM-10A (or SCL-10A/VP) communication bus module and CLASS LC-10AWS (or CLASS−VP) software. HPLC separations were conducted in a Luna 10 C18 (2) (250 mm × 10 mm i.d., 10 μm) semipreparative column (Phenomenex, Torrance, CA) eluted with the system 1 gradient of water and acetonitrile. System 1 consisted of the following: from 0 to 5 min, 5% acetonitrile; from 5 to 30 min, 5−20% acetonitrile; from 30 to 50 min, 20−40% acetonitrile; from 50 to 55 min, 40−100% acetonitrile; from 55 to 65 min, 100−5% acetonitrile.

HPLC/ESI/MS Analyses. On-line HPLC/ESI/MS analyses in the positive mode were carried out using a Quattro II mass spectrometer (Micromass, Manchester, U.K.). A Shimadzu HPLC system (Shimadzu, Kyoto, Japan), consisting of an auto sampler (SIL-10AD/VP), a Rheodyne injector (Cotati, CA), an automated switching valve (FCV-12AH), two pumps (Class LC 10AD), and an SPD-10AV/VP UV detector controlled by a

Table 1. ^{1}H NMR Chemical Shifts of Adducts in DMSO-d_6

Section A: Adduct **A7**[a]

	δ (ppm)		type
H-1′	6.18−6.21	t	N−C*H*O
H-2′	2.55−2.62	m	C*H*$_2$−C
H-2″	2.20−2.25	m	C*H*$_2$−C
H-3′	4.35−4.36	m	HO−C*H*
H-4′	3.81−3.84	m	O−C*H*
H-5′	3.55−3.59	m	HO−C*H*$_2$
H-5″	3.49−3.53	m	HO−C*H*$_2$
OH-5′	4.95−4.96	t	*H*O−CH$_2$
OH-3′	5.27−5.28	d	*H*O−CH
H-2 (1)	8.035	s	N=C*H*−N
H-2 (2)	8.027	s	N=C*H*−N
NH-5	12.16	s (br)	*H*N−C=N
H-6 (1)	6.91	s	C=C*H*−N
H-6 (2)	6.89	s	C=C*H*−N
H-10	6.24−6.27	t	C=C−C*H*−C=C
2H-11	1.98−2.03	m	CH$_2$−C*H*$_2$−CH
2H-12	1.61−1.66	m	CH$_2$−C*H*$_2$−CH$_2$
OH-13	4.37−4.39	t	HO−C*H*$_2$
2H-13	3.44−3.47	m	HO−C*H*$_2$

Section B: Adducts **A8** + **A9**[a]

	δ (ppm)		type
H-1′	6.19−6.22	t	N−C*H*−O
H-2′	2.56−2.59	m	C*H*$_2$−C
H-2″	2.21−2.26	m	C*H*$_2$−C
H-3′	4.35	m	HO−C*H*
H-4′	3.82−3.83	m	O−C*H*
H-5′	3.55−3.59	m	HO−C*H*$_2$
H-5″	3.48−3.53	m	HO−C*H*$_2$
OH-5′	4.92−4.95	t	*H*O−CH$_2$
OH-3′	5.25−5.27	d	*H*O−CH
H-2	8.06	s	N=C*H*−N
NH-5	12.24	s (br)	*H*N−C=N
H-6	7.12	s	C=C*H*−N
H-10	5.73−5.76	t	C=C−C*H*−O
H-11a	2.30−2.33	m	O−CH−C*H*$_2$−CH2
H-11b	1.91−1.94	m	O−CH−C*H*$_2$−CH$_2$
2H-12	1.85−1.90	m	CH$_2$−C*H*$_2$−CH$_2$
H-13a	3.95−3.98	m	CH$_2$−C*H*$_2$−O
H-13b	3.74−3.78	m	CH$_2$−C*H*$_2$−O

[a] Spectra acquired in a DRX 500 NMR spectrometer: m, multiplet; t, triplet; d, doublet; s, singlet.

Table 2. ^{13}C NMR Chemical Shifts of Adducts A7 and A8 + A9 in DMSO-d_6[a]

	A7		**A8 + A9**	
	δ (ppm)	type	δ (ppm)	type
C-2 (1)	136.83	N=*C*H−N	136.91	N=*C*H−N
C-2 (2)	136.77	N=*C*H−N		
C-3a	149.56	C=*C*−*N*	149.77	C=*C*−*N*
C-4a	147.30	N=*C*−*N*	147.17	N=*C*−*N*
C-6	113.40	N−*C*H=C	112.49	N−*C*H=C
C-7 (1)	126.88	C=*C*−*N*	126.48	C=*C*−*N*
C-7 (2)	126.72	C=*C*−*N*		
C-9	153.94	N−*C*=O	153.37	N−*C*=O
C-9a (1)	116.42	C=*C*−*N*	116.14	C=*C*−*N*
C-9a (2)	116.38	C=*C*−*N*		
C-10	33.70	C=C−*C*H−C=C	73.39	C=C−*C*H−O
C-11 (1)	31.36	*C*H$_2$	33.16	*C*H$_2$
C-11 (2)			33.19	*C*H$_2$
C-12	30.75	*C*H$_2$	24.77	*C*H$_2$
C-13	60.86	HO−*C*H$_2$	68.00	CH$_2$−*C*H$_2$−O
C-1′ (1)	83.14	N−*C*H−O	83.05	N−*C*H−O
C-1′ (2)			83.08	N−*C*H−O
C-2′	39.62	*C*H$_2$	39.58	*C*H$_2$
C-3′	70.90	H−*C*−*OH*	70.88	H−*C*−*OH*
C-4′	87.80	H−*C*−*O*	87.80	H−*C*−*O*
C-5′	61.90	H$_2$*C*−*OH*	61.88	H$_2$*C*−*OH*

[a] Spectra were acquired in a DRX 500 spectrometer.

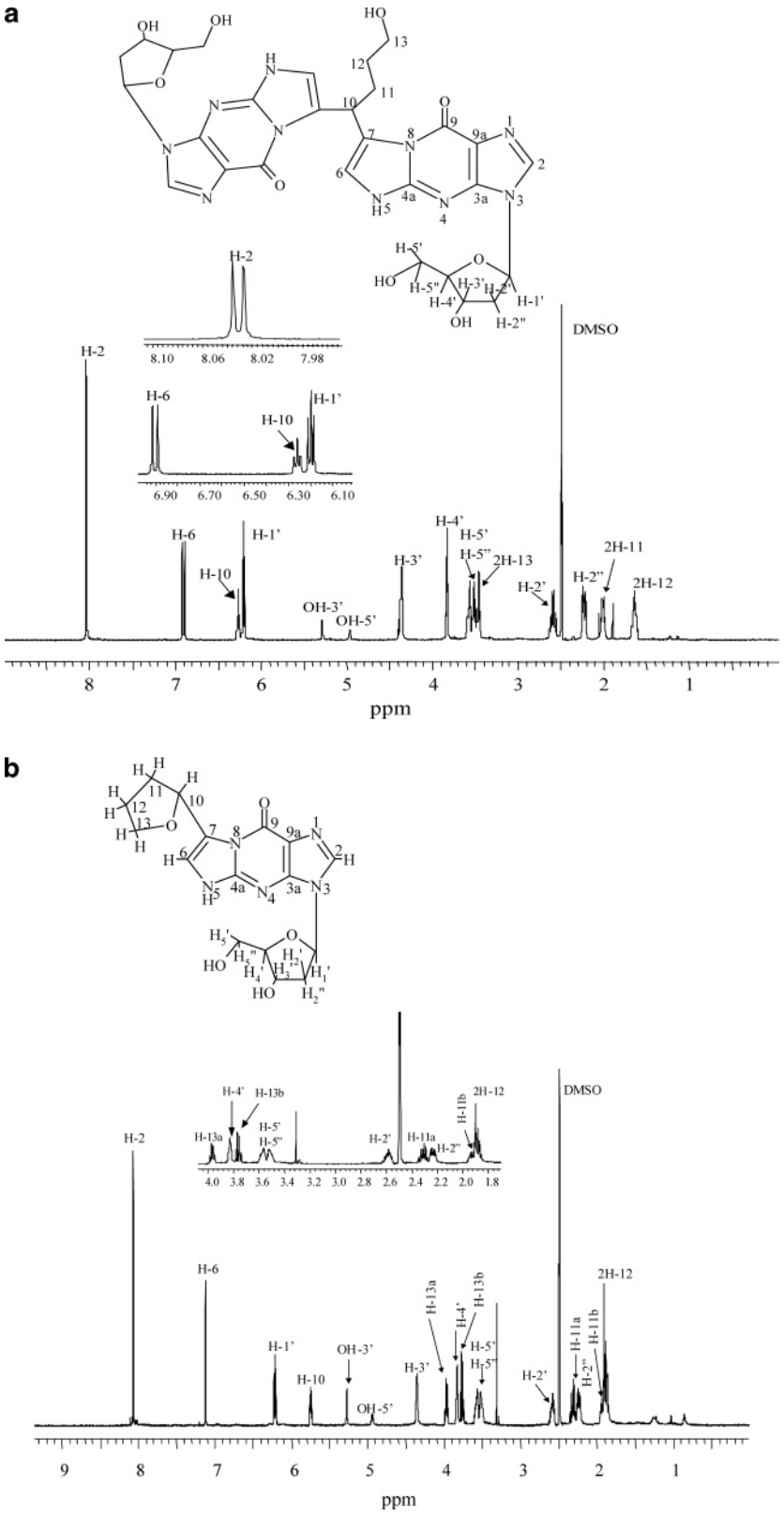

Figure 1. ^{1}H NMR spectra (500.13 MHz) of (a) adduct **A7** and (b) adducts **A8** + **A9** in DMSO-d_6.

communication bus module (SCL-10A/VP−CBM 10A) and Class-VP software, was used for sample injection and cleanup of the analytical column. The source temperature of the mass spectrometer was kept at 100 °C, and flow rates of drying and nebulizing gas (nitrogen) were optimized at 350 and 10 L/h, respectively. The data were processed using MassLynx software (Micromass). Two different HPLC conditions were used, as follows: For system 2, the adducts were eluted from a Luna C18(2) column (250 mm × 4.6 mm i.d., 5 μm, Phenomenex, Torrance, CA) with a gradient of water and acetonitrile (from 0 to 5 min, 10% acetonitrile; from 5 to 30 min, 10−17% acetonitrile; from 30 to 35 min, 17−20% acetonitrile; from 35 to 40 min, 20−30% acetonitrile; from 40 to 45 min, 30−10% acetonitrile) at a flow rate of 0.7 mL/min. After the column, a splitter was connected to allow the entrance of 0.15 mL of the mobile phase into the mass spectrometer. The other 0.55 mL passed through the UV detector (λ = 282 nm). The prepurified samples were dissolved in aqueous solutions containing 0.2% formic acid

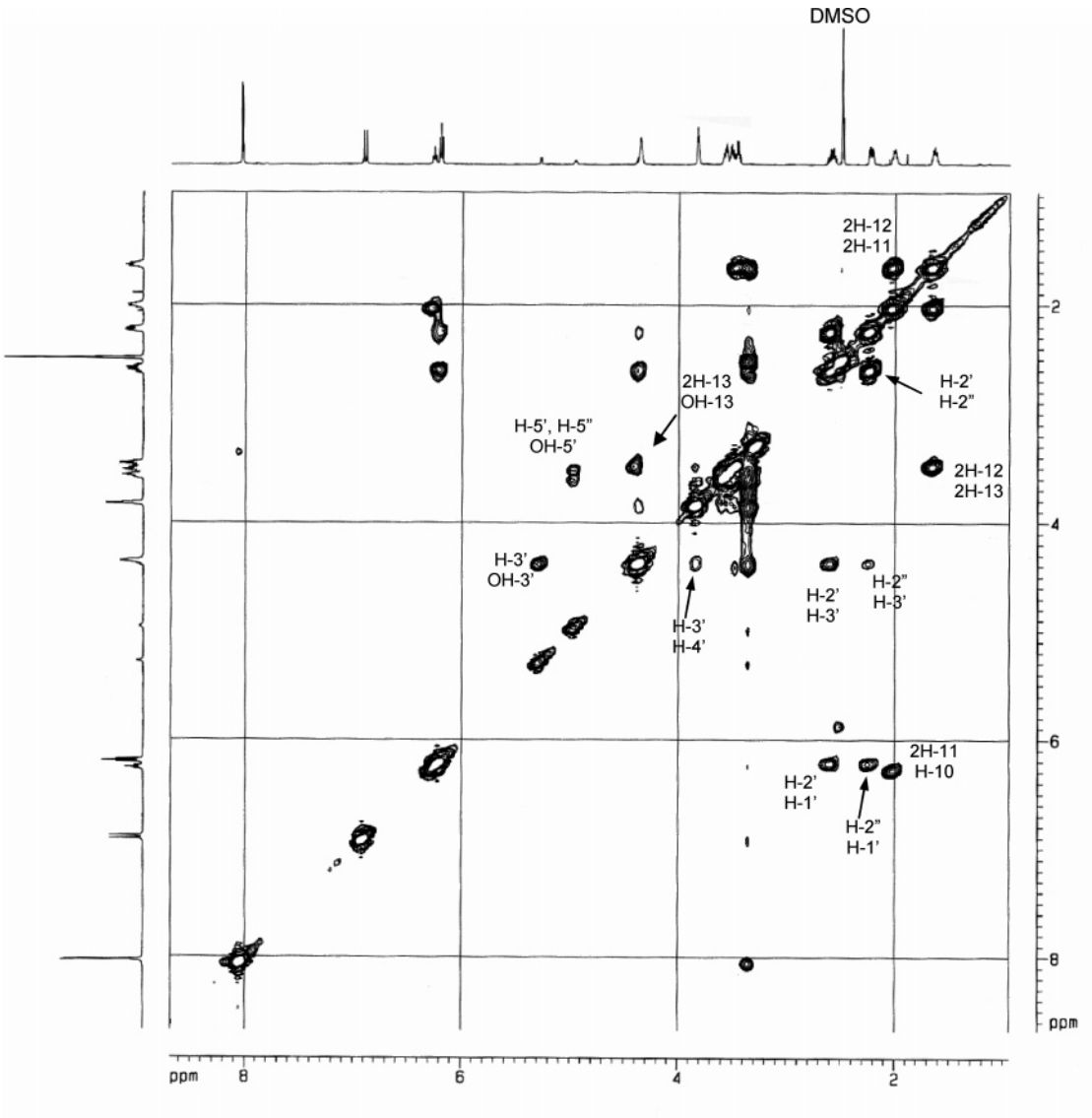

Figure 2. ^{1}H−^{1}H two-dimensional COSY NMR spectrum of adduct **A7** in DMSO-d_6.

(v/v) and injected into the mobile phase through the Rheodyne injector with a 20 μL Rheodyne loop. Full scan data in MS_1 were acquired over a mass range of 100−700 Da with different cone voltages. For system 3, the adducts were eluted from a Luna C18(2) (150 mm × 2 mm i.d., 3 μm, Phenomenex, Torrance, CA) with a gradient of formic acid (0.1% in water) and acetonitrile (from 0 to 5 min, 5% acetonitrile; from 5 to 30 min, 5−20% acetonitrile; from 30 to 50 min, 20−40% acetonitrile; from 50 to 55 min, 40−100% acetonitrile; from 55 to 60 min, 100−5% acetonitrile; from 60 to 70 min, 5% acetonitrile) at a flow rate of 0.12 mL/min. The *m/z* 292 (1,N^2-ϵdGuo), 653 (adduct **A7**), and 362 (adducts **A8** and **A9**) $[M + H]^+$ ions were monitored in the SIR mode with a dwell time of 1 s. The cone voltage was kept at 15 V. Full scan data in MS_1 were collected over a mass range of 100−700 Da with a cone voltage of 30 V.

Preparation and Purification of the Adducts. The α,β-unsaturated aldehyde DDE (28.6 mg, 0.20 mmol) was dissolved in 275 μL of THF, containing 30 μmol of THF−hydroperoxide and 85 μmol of THF−OH, and added to dGuo solutions (5 mg, 0.02 mmol) prepared in 280 μL of 0.2 M carbonate−bicarbonate buffer (pH 9.4). After 48 h of incubation at 50 °C with stirring, the reaction mixtures were extracted twice with one volume of chloroform. The aqueous phase was injected into the HPLC, system 1, for initial 1,N^2-ϵdGuo−THF adducts purification (Figure 1, Supporting Information). The fraction eluted from 21 to 27 min (adducts **A7**−**A9**) was collected and lyophilized. Adducts **A7** and **A8** + **A9** were further purified by HPLC system 1.

Assessment of Adduct Formation from the Reaction of Different α,β-Unsaturated Aldehydes with dGuo in the Presence of Oxidized THF. The α,β-unsaturated aldehydes *trans*-2-octenal (37.8 mg, 0.30 mmol), *trans*-2-nonenal (28 mg, 0.20 mmol), *trans*-2-decenal (30.8 mg, 0.20 mmol), or *trans*,*trans*-2,4-nonadienal (27.6 mg, 0.20 mmol) were dissolved in 275 μL of THF, containing 30 μmol of THF-hydroperoxide and 85 μmol of THF−OH, and added to dGuo solutions (5 mg, 0.02 mmol) prepared in 280 μL of 0.2 M carbonate−bicarbonate buffer (pH 11). After 48 h of incubation at 50 °C under stirring, the reaction mixtures were extracted twice with one volume of chloroform. The aqueous phase was injected into the HPLC/ESI/MS system 3 for analysis.

Assessment of Adduct Formation from the Reaction of Oxidized THF with 1,N^2-ϵdGuo. The adduct 1,N^2-ϵdGuo (0.007 mg, 25 nmol) was dissolved in 110 μL of 0.2 M carbonate−bicarbonate buffer (pH 9.4) and incubated with THF containing 0.52 μmol of THF−hydroperoxide and 1.47 μmol of THF−OH for 24 h at 37 °C. The reaction mixture was then extracted with one volume of chloroform, and the aqueous phase was injected into the HPLC/ESI/MS system 3 for analysis.

pH Stability of Adducts A7−A9. The isolated adducts **A7** and **A8** + **A9** were incubated at pH 4.0 (0.05 M acetate buffer), pH 7.4 (0.05 M phosphate buffer), and pH 11.0 (0.05 M

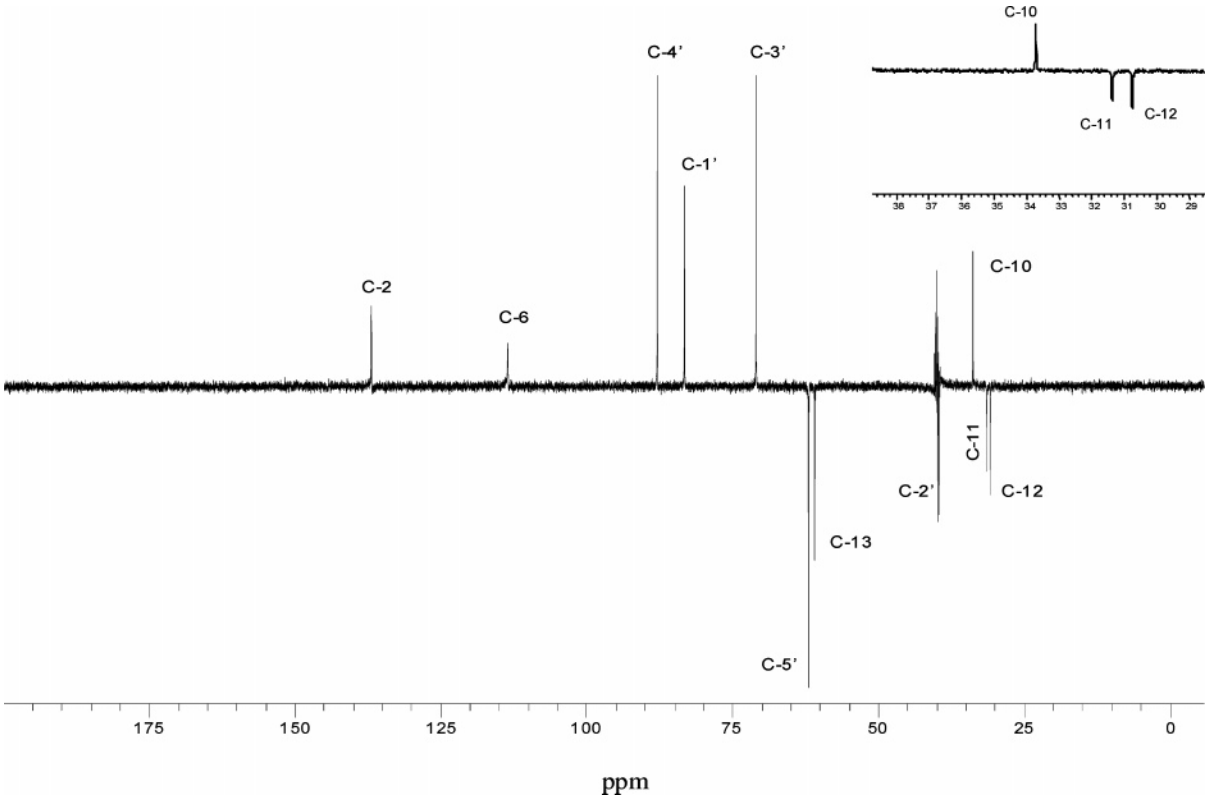

Figure 3. DEPT NMR spectrum of adduct **A7** in DMSO-d_6.

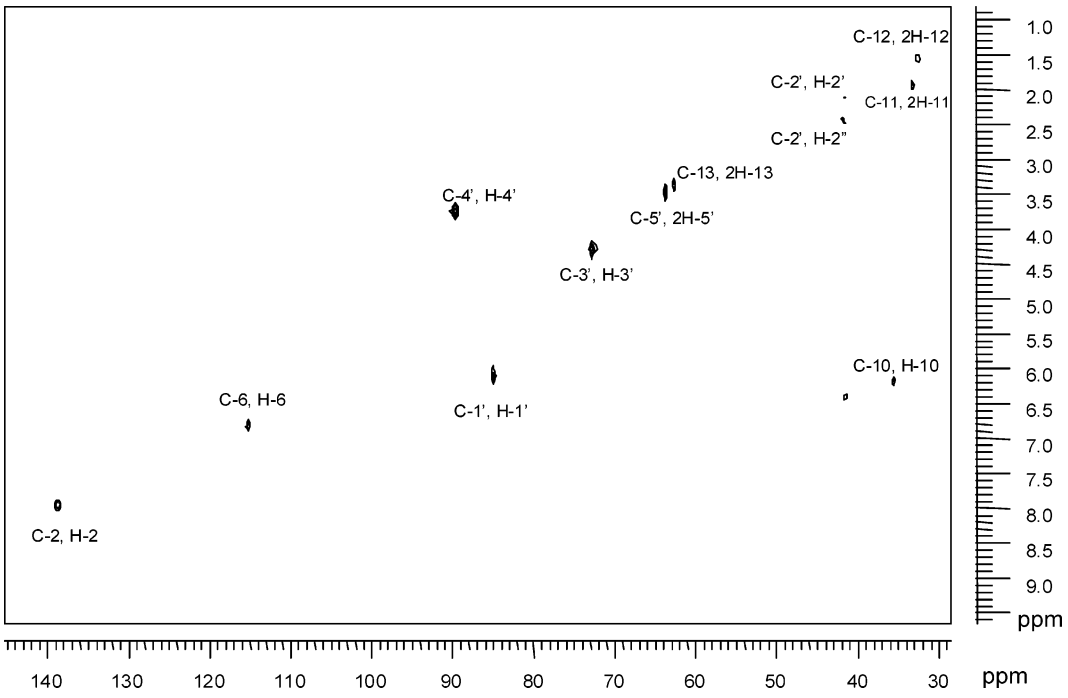

Figure 4. ^{1}H−^{13}C two-dimensional HMQC spectrum of adduct **A7** in DMSO-d_6.

carbonate−bicarbonate buffer) for 15 min, 1 h, 5 h, and 24 h at 37 °C. After the incubation period, a fraction was analyzed by HPLC/ESI/MS system 3, as described above.

Characterization of the Adducts. The adducts were characterized by UV, ESI/MS, ^{1}H NMR, and ^{13}C NMR spectra analyses. The UV spectra of adducts **A7** and **A8** + **A9** are illustrated in Figure 2, Supporting Information. The positive mode ESI/MS analysis of adduct **A7** (Figure 3A, Supporting Information) shows five important signals at *m/z* 653 ($[M + H]^+$, 10% relative intensity), *m/z* 537 ($[M + H]^+ - 2$-D-*erythro*-pentose, 30% relative intensity), *m/z* 421 ($[M + H]^+ - 2$-D-*erythro*-pentose − 2-D-*erythro*-pentose, 100% relative intensity), *m/z* 246 ($[M + H]^+ - 2$-D-*erythro*-pentose − 1,N^2-ϵdGuo, 72% relative intensity), and *m/z* 176 ([1,N^2-ϵGua + H]$^+$, 40% relative intensity). The positive mode ESI/MS spectra of adducts **A8** and **A9** (Figure 3B, Supporting Information) show two important signals at *m/z* 362 ($[M + H]^+$, 17% relative intensity) and *m/z* 246 ($[M + H]^+ - 2$-D-*erythro*-pentose, 100% relative intensity). Figure 1 shows the ^{1}H NMR spectra of adducts **A7** and **A8** + **A9**, while Figure 2 presents the ^{1}H−^{1}H COSY spectrum of adduct **A7** and Figure 4, Supporting Information, presents the ^{1}H−^{1}H COSY spectrum of adducts **A8** + **A9**. Table 1, sections

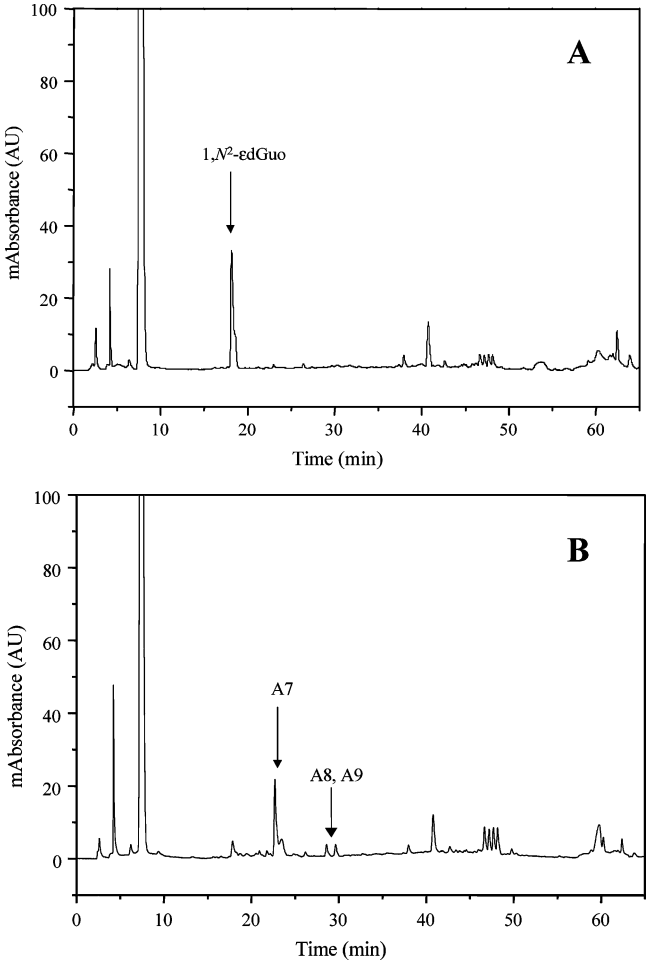

Figure 5. HPLC elution profile of the reaction mixture of dGuo with DDE in the presence of (a) distilled THF and (b) oxidized THF. The chromatograms were obtained with HPLC system 1 ($\lambda = 285$ nm). Conditions were as described in the Experimental Procedures section.

A and B, summarizes the ^{1}H NMR data of the adducts, while Table 2 gives the ^{13}C NMR data.

Results

Reaction of dGuo with *trans,trans*-2,4-Decadienal in the Presence of Oxidized THF. We have already shown that the reaction of dGuo with DDE at pH 9.4 in the presence of THF containing hydroperoxides leads to the formation of several products, which can be separated by HPLC system 1 (Figure 1, Supporting Information) (*7*). Adducts **A1**−**A6** were previously characterized as etheno and hydroxy-ethano adduct derivatives resulting from the reaction of the hydroperoxide-oxidized aldehyde with dGuo (*7*, *8*). The present work focused on elucidating the structures of adducts **A7**−**A9**, which exhibit retention times at 21−27 min and, unlike the other products, are observed only when the reactions occur in the presence of oxidized THF.

Purification and Spectroscopic Characterization of the Adducts. Adducts **A7**−**A9** were purified by eluting the aqueous phase of the reaction mixture through the HPLC system 1. The collected fractions were concentrated under vacuum and repurified through the same HPLC system. We attempted, unsuccessfully, to separate adduct **A8** from adduct **A9**, because they interconvert after the isolation procedure.

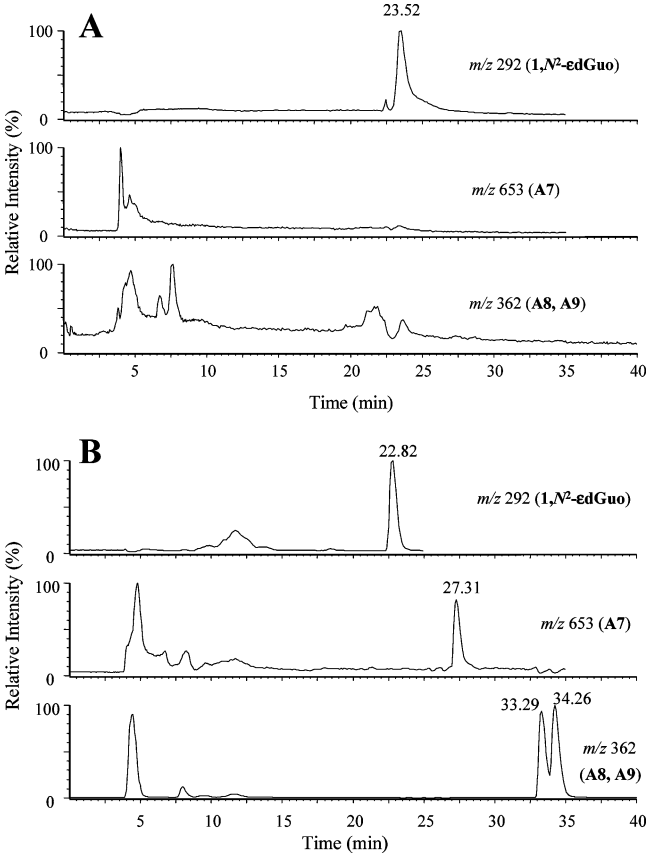

Figure 6. HPLC elution profile with ESI/MS (SIR) detection of the ions $[M + H]^+$ *m/z* 292 (1,N^2-ϵdGuo), 653 (**A7**), and 362 (**A8**, **A9**) of (a) purified 1,N^2-ϵdGuo and (b) 1,N^2-ϵdGuo reacted with oxidized THF. The chromatograms were obtained with HPLC system 3. Conditions were as described in the Experimental procedures section.

The three adducts display similar UV spectra with λ_{max} at 229 and 287 nm (pH 7.4) for adduct **A7** and λ_{max} at 228 and 282 nm (pH 7.4) for adducts **A8** + **A9** (Figure 2, Supporting Information). The UV spectra obtained for adducts **A8** and **A9** through the photodiode array detector coupled to the HPLC system 1 are identical (data not shown). This UV feature indicates an etheno-2′-deoxyguanosine structure, as described previously (*7*).

The ESI/MS spectrum of adduct **A7** (Figure 3A, Supporting Information) shows a protonated molecular ion $[M + H]^+$ at *m/z* 653 ($[M + H]^+$, 10% relative intensity), a predominant fragment ion at *m/z* 421 ($[M + H]^+ - 2$-D-*erythro*-pentose − 2-D-*erythro*-pentose, 100% relative intensity), and three other signals at *m/z* 537 ($[M + H]^+$ − 2-D-*erythro*-pentose, 30% relative intensity), *m/z* 246 ($[M + H]^+ - 2$-D-*erythro*-pentose − 1,N^2-ϵdGuo, 72% relative intensity), and *m/z* 176 ([1,N^2-ϵGua + H]$^+$, 40% relative intensity). These ascriptions are consistent with the formation of a dimer of 1,N^2-ϵdGuo linked to a THF molecule. The positive mode ESI/MS spectra of adducts **A8** and **A9** (Figure 3B, Supporting Information) are identical and show a protonated molecular ion $[M + H]^+$ at *m/z* 362 ($[M + H]^+$, 17% relative intensity) and a predominant fragment ion at *m/z* 246 ($[M + H]^+ - 2$-D-*erythro*-pentose, 100% relative intensity). The MS data indicate an increase in the molecular mass of the adducts by 70 Da with respect to 1,N^2-ϵdGuo, being consistent with an adduct 1,N^2-ϵdGuo/THF (1:1) with the loss of two hydrogen atoms. The identical UV and mass spectral

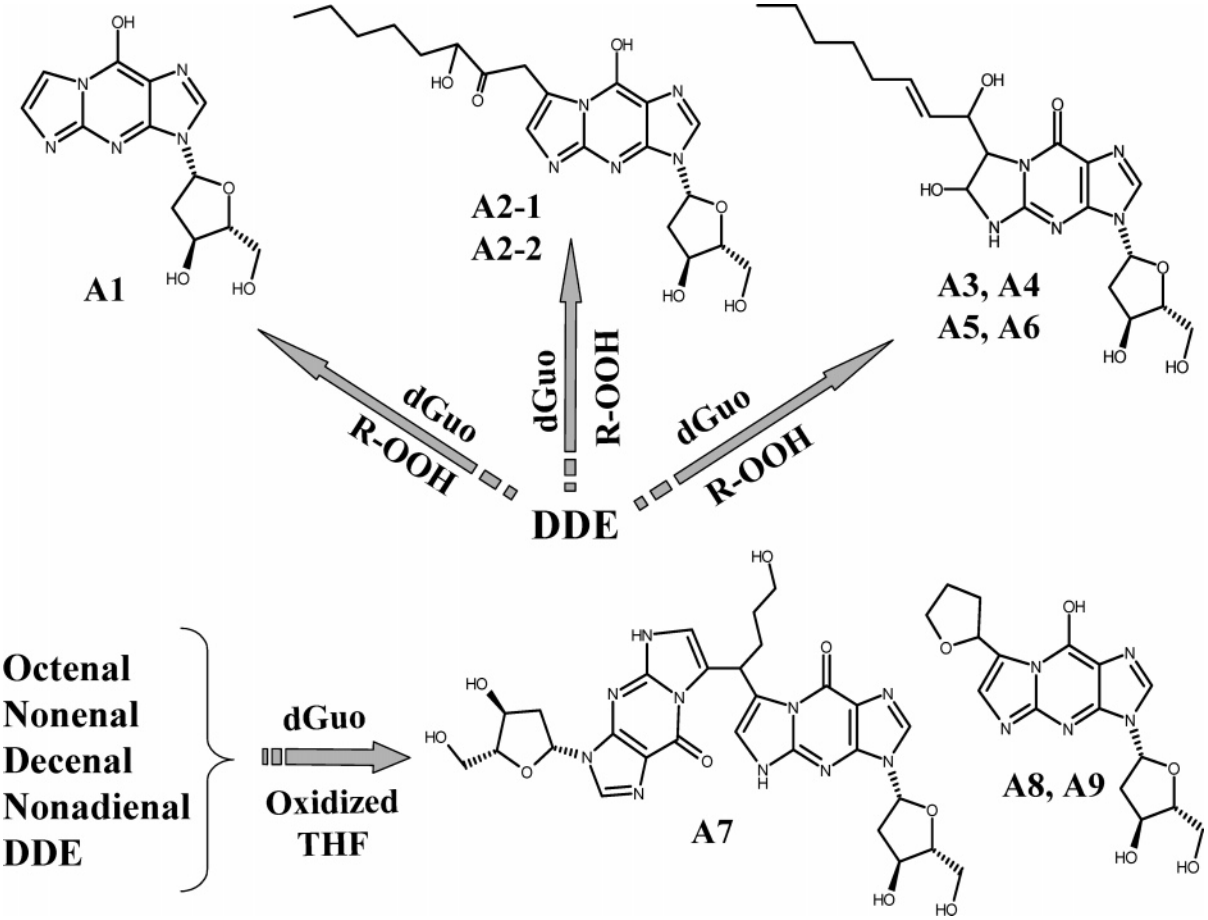

Figure 7. Structures and sources of adducts **A1**−**A9**.

features of adducts **A8** and **A9** indicate that they are isomeric products.

The molecular structures of these adducts were further confirmed by ^{1}H NMR 1D (Figure 1 and Table 1, sections A and B), 2D (Figure 2 and Figure 4, Supporting Information), ^{13}C NMR (Table 2), DEPT (Figure 3 and Figure 5, Supporting Information), and HMQC (Figure 4 and Figure 6, Supporting Information) spectral analysis. The ^{1}H NMR (Figure 1) and ^{1}H−^{1}H COSY (Figure 2) spectra of adduct **A7** in DMSO-d_6 show, in addition to the sugar protons, a pair of singlets at 8.035 and 8.027 ppm (H-2) and another at 6.91 and 6.89 ppm (H-6). Peak integration revealed that nearly all the protons were present in duplicate, with the exception of those at 6.26 ppm (H-10) and 4.38 ppm (OH-13). The signals at 1.64 ppm (2H-12), 2.00 ppm (2H-11), 3.45 ppm (2H-13), 4.38 ppm (OH-13), and 6.26 ppm (H-10) indicate the presence of an alkyl side chain in the structure, probably being the link between two 1,N^2-ϵdGuo residues. The ^{13}C NMR spectrum displays 16 signals corresponding to 16 different carbon atoms. Some of these signals (C-2, C-7, C-9a) are duplicated, one of each coming from the respective carbon in each 1,N^2-ϵdGuo residue of the double adduct (Table 2). DEPT and HMQC (Figures 3 and 4) indicate that C-2, C-6, and C-10 are −CH groups and that C-11, C-12, and C-13 are $-CH_2$ groups. The signals at 60.86 ppm (C-13) and 3.45 ppm (2H-13) lie within the characteristic range of carbon linked to an −OH group and protons linked to a −COH group, respectively. A correlation between the signals at 4.38 ppm (OH-13) and 3.45 ppm (2H-13) is observed in the two-dimensional COSY spectrum, besides the correlations between the signals at 3.45 ppm (2H-13) and 1.64 ppm (2H-12), 1.64 ppm (2H-12) and 2.00 ppm (2H-11), and 2.00 ppm (2H-11) and 6.26 ppm (H-10) (Figure 2). The chemical shifts of H-10 (6.26 ppm) and C-10 (33.70 ppm) are in agreement with those described by Golding and co-workers (*10*), who characterized a similar structure (a dimer of 1,N^2-ϵdGuo) resulting from the reaction of dGuo with glycidaldehyde.

The ^{13}C NMR spectrum of adducts **A8** + **A9** also displays 16 signals corresponding to 16 different carbon atoms (Table 2). Comparing the ^{13}C NMR spectra of adducts **A7** and **A8** + **A9**, we can see that the signal at 33.70 ppm (C-10, **A7**) is not present in the spectrum of **A8** + **A9**. Additionally, there is a signal at 73.39 ppm that is absent from the spectrum of **A7** and lies within the characteristic range of carbon linked to an oxygen atom. Another signal appears at 67.99 ppm (C-13), also falling within the characteristic range of carbon linked to oxygen. DEPT and HMQC (Figures 5 and 6, Supporting Information) indicate that C-11 (33.16 ppm for one isomer and 33.19 ppm for the other), C-12 (24.77 ppm), and C-13 (67.99 ppm) are $-CH_2$ groups and that C-10 (73.39 ppm) is a −CH group. The chemical shifts of these carbon atoms are congruent with those described to the THF molecule (NMR tables in the literature). The ^{1}H NMR (Figure 1B) and ^{1}H−^{1}H COSY (Figure 4, Supporting Information) spectra of adducts **A8** + **A9** in DMSO-d_6 show, in addition to the sugar protons, the singlets at 8.06 ppm (H-2) and 7.12 ppm (H-6), pointing to a substituted 1,N^2-ϵdGuo structure. The correlations between the signals at 5.74 ppm (H-10), 2.31 ppm (H-11a), and 1.92 ppm (H-11b); at 2.31 ppm (H-11a), 1.92 ppm (H-11b), and 1.87 ppm (2H-12); and at 1.87 ppm (2H-

Scheme 1. Structures and Proposed Mechanism for Formation of Adducts A7−A9

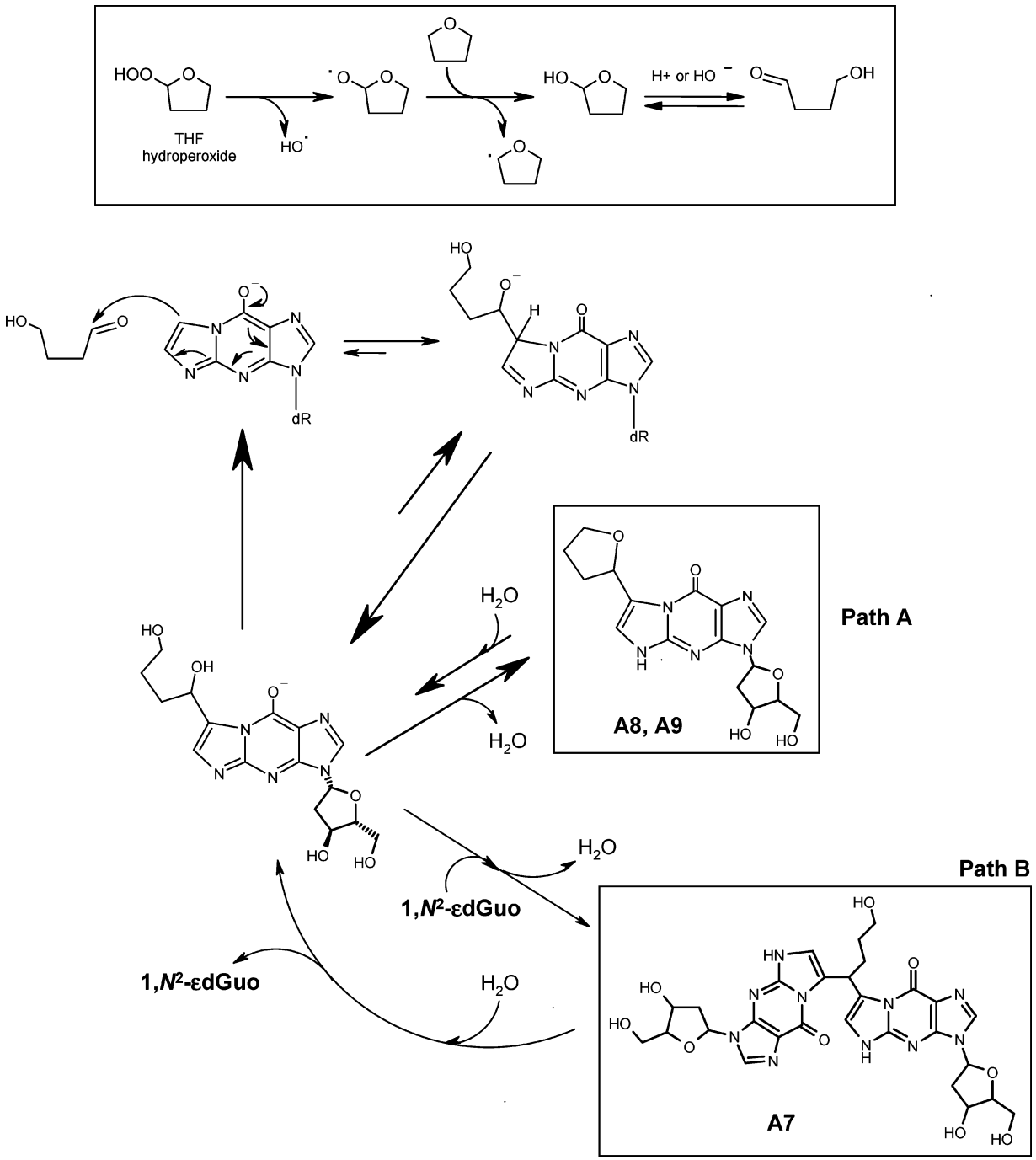

12), 3.96 ppm (H-13a), and 3.76 ppm (H-13b) are observed in the two-dimensional COSY spectrum. The chemical shifts of H-12 and H-13 protons are also congruent with those described for the THF molecule (NMR tables in the literature).

Taken together, the above data can be rationalized as follows: adduct **A7** consists of two 1,N^2-ϵdGuo residues linked to a hydroxy-carbon side chain; adducts **A8** and **A9** are interconvertible 1,N^2-ϵdGuo derivatives bearing a THF moiety.

pH Stability of the Adducts. The isolated adducts **A7** and **A8** + **A9** were incubated under pH 4.0, 7.4, and 11.0 at 37 °C, and their stability was analyzed by the magnitude of the signals in the HPLC/ESI/MS system 3 up to 24 h. The three adducts are stable at pH 4.0 (data not shown). We observed a decrease of **A7**, **A8**, and **A9** stability with the increase of pH and time of incubation. Adduct **A7** gives rise to **A8**, **A9**, and 1,N^2-ϵdGuo upon incubation at pH 7.4 and 11, as illustrated in Figure 7A, Supporting Information. Adducts **A8** and **A9** decompose to 1,N^2-ϵdGuo at pH 7.4 and 11, as illustrated in Figure 7B, Supporting Information.

Adduct Formation from the Reaction of Other α,β-Unsaturated Aldehydes with dGuo in the Presence of Oxidized THF. We observed that not only DDE but other α,β-unsaturated aldehydes (2-octenal, 2-nonenal, 2-decenal, and 2,4-nonadienal) also lead to adducts **A7**, **A8**, and **A9** upon incubation with dGuo in the presence of oxidized THF (data not shown). As in the case of DDE, adducts were detected only in the reactions occurring in the presence of THF oxidation products. Incubations with distilled THF (initially without hydro-

peroxides) did not lead to **A7**−**A9** formation (Figure 5).

Adduct Formation from the Reaction of 1,N^2-ϵdGuo with Oxidized THF. The previous observations point to a reaction between 1,N^2-ϵdGuo and a THF oxidation product for the formation of adducts **A7**−**A9**. In fact, when the isolated adduct 1,N^2-ϵdGuo was incubated with oxidized THF, as described in the Experimental Procedures section, an analysis by the HPLC/ESI/MS system 3 revealed the formation of adducts **A7**−**A9** (Figure 6).

Discussion

We have recently shown that the reaction of dGuo with *trans*,*trans*-2,4-decadienal (DDE), a highly cytotoxic aldehyde generated as a product of lipid peroxidation in cell membranes, results in the formation of a number of different base derivatives. Seven adducts were fully characterized (*7*, *8*): adduct **A1** is 1,N^2-ϵdGuo, a well-known reaction product of epoxy aldehydes with dGuo, adducts **A2**−**1** and **A2**−**2** are 1,N^2-ϵdGuo adducts possessing a carbon side chain with a carbonyl and a hydroxyl group, and adducts **A3**−**A6** are four diastereoisomeric 1,N^2-hydroxyethano-dGuo derivatives possessing a carbon side chain with a double bond and a hydroxyl group (Figure 7).

In this study, an analysis of the reaction between DDE and dGuo performed in THF revealed the formation of three novel adducts designated **A7**, **A8**, and **A9**. Thus, 3-(2′-deoxy-β-D-*erythro*-pentafuranosyl)-7-[3-hydroxy-1-(3-(2′-deoxy-β-D-*erythro*-pentafuranosyl)-3,5-dihydro-imidazo-[1,2-*a*]purin-9-one-7-yl)-propyl]-3,5-dihydro-imidazo[1,2-*a*]purin-9-one (adduct **A7**) and 3-(2′-deoxy-β-D-*erythro*-pentafuranosyl)-7-(tetrahydro-furan-2-yl)-3,5-dihydro-imidazo[1,2-*a*]purin-9-one (adducts **A8** and **A9**) were characterized on the basis of extensive spectroscopic measurements. Unlike adducts **A1**−**A6**, adducts **A7**−**A9** were only observed in the reactions carried out in the presence of THF. The three adducts are products of the combination of 1,N^2-ϵdGuo and oxidized THF. Adduct **A7** consists of two 1,N^2-ϵdGuo residues linked to a hydroxy-carbon side chain. Adducts **A8** and **A9** are interconvertible 1,N^2-ϵdGuo derivatives bearing a THF moiety. Reactions performed in the presence of other α,β-unsaturated aldehydes (2-octenal, 2-nonenal, 2-decenal, and 2,4-nonadienal) and THF also give rise to **A7**−**A9** adducts.

Adducts **A7**−**A9** undergo slow decomposition at pH 7.0 and 11.0. Adducts **A8** and **A9** go back to 1,N^2-ϵdGuo, while adduct **A7** leads to **A8** and **A9** with the concomitant release of 1,N^2-ϵdGuo.

The proposed reaction mechanism yielding adducts **A7**−**A9** is shown in Scheme 1. This mechanism involves the electrophilic attack on 1,N^2-ϵdGuo by the carbonyl of 4-hydroxy-butanal, generated via ring opening of α-hydroxy-THF (THF−OH), giving adducts **A8** and **A9** (path A). Hydroxyalkylation (*11*, *12*) of another 1,N^2-ϵdGuo by either of these adducts, or by their diol precursor, produces the double adduct **A7** (path B).

Double structures involving the 1,N^2-ϵdGuo adduct have already been described by Golding and co-workers (*10*) in the reaction of glycidaldehyde, classified as an animal carcinogen, with dGuo. *N*-Nitrosopyrrolidine, a cyclic nitrosamine generated endogenously and present in the diet and in cigarette smoke, is metabolically activated to the α-hydroxyl derivative, which further reacts with dGuo, yielding a THF−dGuo adduct as one of the main products in in vitro reactions (*13*). One of the major products of the solvolysis of the in vitro α-hydroxynitrosamine precursor, α-acetoxy-*N*-nitrosopyrrolidine, is the intermediate THF−OH, which is involved in one of the mechanisms for THF−dGuo formation (*13*).

Several reports have described the formation of adducts from nucleosides and aldehydes produced during the lipid peroxidation process (*14*, *15*). Our results indicate the formation of condensation adducts between 1,N^2-ϵdGuo and THF oxidation products. This pathway can be relevant in studies on nucleoside adduct formation using THF as solvent. Moreover, considering the formation of THF−OH from α-acetoxy-*N*-nitrosopyrrolidine (*13*) and the detection of γ-hydroxybutyric acid in human biological fluids in a case of acute THF poisoning (*3*), one could expect the potential formation of the present adducts under conditions in which humans are exposed to oxidative stress and THF−OH sources. Further studies are required to verify the relevance of this mechanism in vivo.

Acknowledgment. This work was supported by the Fundação de Amparo à Pesquisa do Estado de São Paulo, FAPESP (Brazil), the Conselho Nacional para o Desenvolvimento Científico e Tecnológico, CNPq (Brazil), Pró-Reitoria de Pesquisa da Universidade de São Paulo (Brazil), and Programa de Apoio aos Núcleos de Excelência, PRONEX/FINEP (Brazil). A.P.M.L. held a FAPESP fellowship, E.P.M.P. holds a FAPESP fellowship, and O.F.G. holds a CNPq fellowship. P.D.M. is the recipient of a fellowship from the Guggenheim Foundation.

Supporting Information Available: Figure 1: HPLC elution profile of the reaction mixture of dGuo with DDE in the presence of oxidized THF. The chromatogram was obtained with HPLC system 1. Conditions as described in the Experimental Procedures section. Figure 2: UV absorption spectra of (a) adduct **A7** and (b) adducts **A8** + **A9** at different pH (pH 1, 50 mM HCl-KCl; pH 7, 50 mM phosphate buffer; pH 11, 50 mM carbonate−bicarbonate buffer). Conditions as described in the Experimental Procedures section. Figure 3: ESI/MS spectra of (a) adduct **A7** and (b) adducts **A8** and **A9**. Cone voltage was 50 V. Conditions as described in the Experimental Procedures section. Figure 4: ^{1}H−^{1}H two-dimensional COSY NMR spectrum of adducts **A8** + **A9** in DMSO-d_6. Figure 5: DEPT NMR spectrum of adducts **A8** + **A9** in DMSO-d_6. Figure 6: ^{1}H−^{13}C two-dimensional HMQC spectrum of adducts **A8** + **A9** in DMSO-d_6. Figure 7: HPLC elution profile with ESI/MS (SIR) detection of the ions $[M + H]^+$ *m/z* 292 (1,N^2-ϵdGuo), 653 (**A7**), and 362 (**A8**, **A9**) of (a) purified adduct **A7** incubated in 0.05 M phosphate buffer (pH 7.4) for 15 min, 5 h, and 24 h and (b) purified adducts **A8** + **A9** incubated in 0.05 M phosphate buffer (pH 7.4) for 15 min, 5 h, and 24 h. The chromatograms were obtained with HPLC system 3. Conditions as described in the Experimental Procedures section. This material is available free of charge via the Internet at http://pubs.acs.org.

References

(1) Ong, C. N., Chia, S. E., Phoon, W. H., and Tan, K. T. (1991) Biological monitoring of occupational exposure to tetrahydrofuran. *Br. J. Ind. Med. 48*, 616−621.

(2) Hazardous Substances Data Bank (HSDB) (2003) Database maintained by the National Library of Medicine, available through the MEDLARS system. U.S. Department of Health and Human Services, Public Health Service, National Institutes of Health, Bethesda, MD.

(3) Cartigny, B., Azaroual, N., Imbenotte, M., Sadeg, N., Testart, F., Richecoeur, J., Vermeersch, G., and Lhermitte, M. (2001) ^{1}H NMR spectroscopic investigation of serum and urine in a case of acute tetrahydrofuran poisoning. *J. Anal. Toxicol. 25*, 270−274.

(4) National Toxicology Program (NTP) (1998) Toxicology and carcinogenesis studies of tetrahydrofuran (CAS No. 109-99-9) in F344/N rats and B6C3F1 mice. Technical Report Series No. 475, NIH Publication No. 98-3965, U.S. Department of Health and Human Services, Public Health Service, National Institutes of Health, Research Triangle Park, NC.
(5) Chhabra, R. S., Herbert, R. A., Roycroft, J. H., Chou, B., Miller, R. A., and Renne, R. A. (1998) Carcinogenesis studies of tetrahydrofuran vapors in rats and mice. *Toxicol. Sci. 41*, 183−188.
(6) American Conference of Governmental Industrial Hygienists (ACGIH) (2002) *TLVs and BEIs: Threshold limit Values for Chemical Substances and Physical Agents and Biological Exposure Indices for 2002*, Cincinnati, OH.
(7) Loureiro, A. P. M., Di Mascio, P., Gomes, O. F., and Medeiros, M. H. G. (2000) *trans*,*trans*-2,4-Decadienal-induced 1,N^2-etheno-2′-deoxyguanosine adduct formation. *Chem. Res. Toxicol. 13*, 601−609.
(8) Loureiro, A. P. M., Campos, I. P. d. A., Gomes, O. F., Di Mascio, P., and Medeiros, M. H. G. (2004) Structural characterization of diastereoisomeric ethano adducts derived from the reaction of 2′-deoxyguanosine with *trans*,*trans*-2,4-decadienal. *Chem. Res. Toxicol. 17*, 641−649.
(9) Jiang, Z.-Y., Woollard, A. C. S., and Wolff, S. P. (1991) Lipid hydroperoxide measured by oxidation of Fe^{2+} in the presence of xylenol orange. Comparison with the TBA assay and an iodometric method. *Lipids 26*, 853−856.
(10) Golding, B. T., Slaich, P. K., Kennedy, G., Bleasdale, C., and Watson, W. P. (1996) Mechanisms of formation of adducts from reactions of glycidaldehyde with 2′-deoxyguanosine and/or guanosine. *Chem. Res. Toxicol. 9*, 147−157.
(11) Schnell, H., and Krimm, H. (1963) Formation and cleavage of dihydroxydiarylmethane derivatives. *Angew. Chem., Int. Ed. Engl. 2*, 373−379.
(12) Casiraghi, G., Casnati, G., Pochini, A., Puglia, G., Ungaro, R., and Sartori, G. (1981) Uncatalyzed phenol-formaldehyde reactions. A convenient synthesis of substituted 2,2′-dihydroxydiphenylmethanes. *Synthesis* 143−146.
(13) Young-Sciame, R., Wang, M., Chung, F. L., and Hecht, S. S. (1995) Reactions of alpha-acetoxy-*N*-nitrosopyrrolidine and alpha-acetoxy-*N*-nitrosopiperidine with deoxyguanosine: formation of N^2-tetrahydrofuranyl and N^2-tetrahydropyranyl adducts. *Chem. Res. Toxicol. 8*, 607−616.
(14) Marnett, L. J., Riggins, J. N., and West, J. D. (2003) Endogenous generation of reactive oxidants and electrophiles and their reactions with DNA and protein. *J. Clin. Invest. 111*, 583−593.
(15) Bartsch, H., Nair, J., and Owen, R. W. (2002) Exocyclic DNA adducts as oxidative stress markers in colon carcinogenesis: potential role of lipid peroxidation, dietary fat and antioxidants. *Biol. Chem. 383*, 915−921.

TX0497494